

## Introduction

Physiologically-based pharmacokinetic (PBPK) models mechanistically describe a drug's distribution in the body. Bayesian analysis integrates prior knowledge and data to make inferences on model parameters. Bayesian PBPK modeling takes advantage of the relatively strong prior mechanistic knowledge of the system of interest while quantifying the uncertainty around the model parameters.

This study demonstrates convenient, open-source Bayesian PBPK modeling frameworks in R and Julia. The results from this approach were validated against the reported results from a previously developed model [1].

## Methods

A full body population Bayesian PBPK model was built for the drug, mavoglurant, in R/Stan and Julia/Turing.jl. The model structure is shown in Figure 1 and was largely based on a previously developed model that was later implemented in the R package, nlmixr [1, 2]. The open-source library, Torsten, was used to facilitate Stan's handling of pharmacometric data. The PBPK model was defined in Julia using the SciML open-source tools. Bayesian inference of the parameters of interest was carried out by running the No U-Turn Sampler (NUTS) on 4 different chains. Within-chain parallelization was utilized to speed up run times. Three different implementations were run: general and linear ordinary differential equation (ODE) solver runs in Stan/Torsten, and a general ODE run in SciML/Turing.jl.

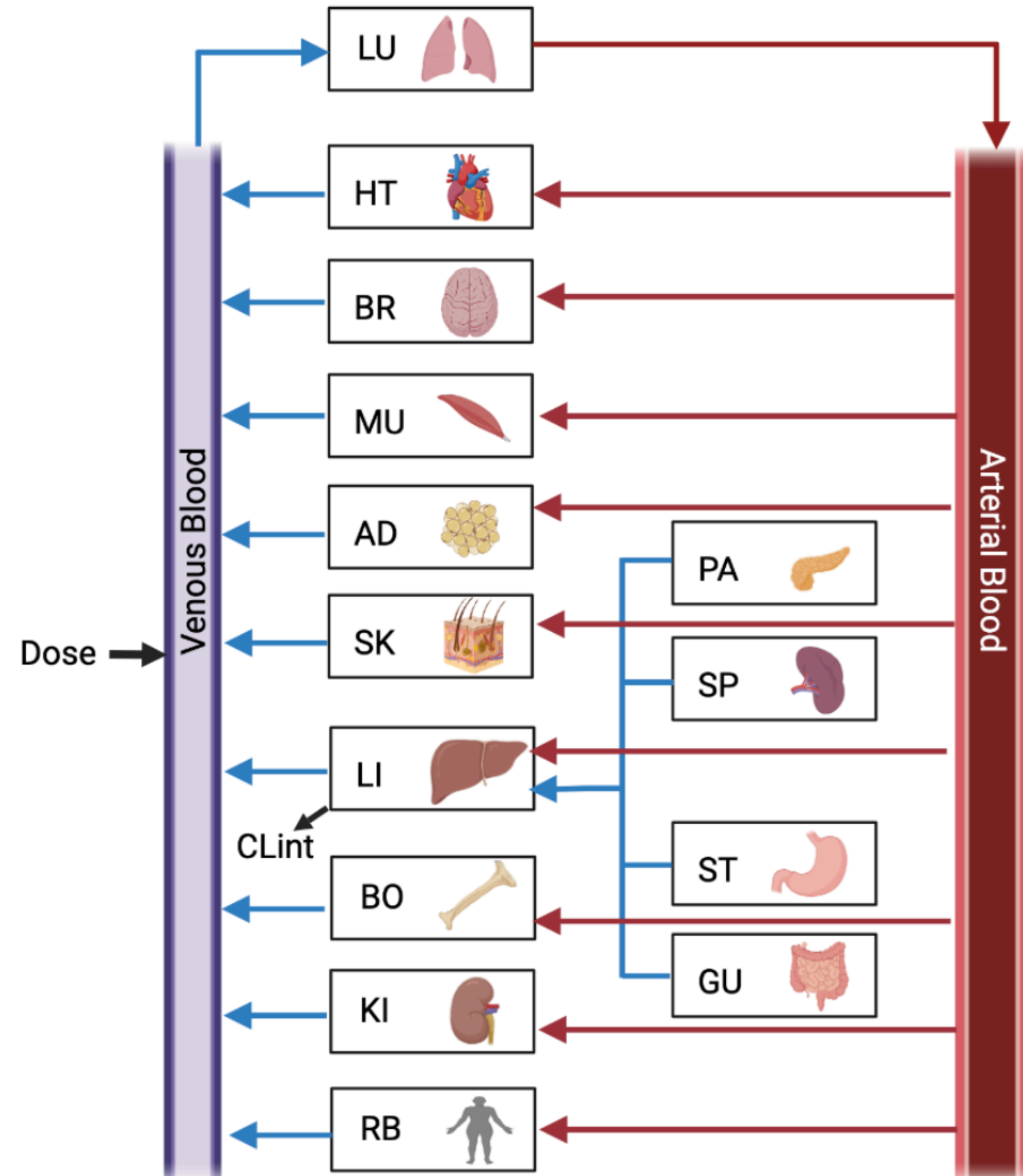


**Figure 1. PBPK Model Structure.** LU, HT, BR, MU, AD, SK, LI, BO, KI, PA, SP, ST, GU, RB refer to lung, heart, brain, muscle, adipose, skin, liver, bone, kidney, pancreas, spleen, stomach, gut, and rest of body, respectively. CLint is intrinsic clearance.

### General PBPK Model Equations:

#### Non-eliminating organ:

$$\frac{dA_T}{dt} = Q_T(C_A - \frac{C_T}{Kb_T}) \quad (1)$$

#### Eliminating organ:

$$\frac{dA_T}{dt} = Q_T(C_A - \frac{C_T}{Kb_T}) - CL * f_{ub} * C_T / Kb_T \quad (2)$$

#### Lung:

$$\frac{dA_{LU}}{dt} = Q_{LU}(C_V - \frac{C_{LU}}{Kb_{LU}}) \quad (3)$$

#### Arterial blood:

$$\frac{dA_A}{dt} = Q_{LU}(\frac{C_{LU}}{Kb_{LU}} - C_A) \quad (4)$$

#### Venous blood:

$$\frac{dA_V}{dt} = \sum_T (Q_T * C_T / Kb_T) - Q_{LU} * C_V \quad (5)$$

A=amount; C=concentration; Q=blood flow; Kb=partition coefficient; CL=clearance;  $f_{ub}$ =unbound fraction in blood; subscripts T, A, V, and LU refer to tissue, arterial blood, venous blood, and lung, respectively.

#### Statistical Model:

$$\log(c_{ij}) = N(\log(\hat{c}_{ij}), \sigma^2) \quad (6)$$

$$\hat{c}_{ij} = f_{PBPK}(t_{ij}, D_i, p_i) \quad (7)$$

$$p_i = [\theta_i, v_i] \quad (8)$$

$$\theta_i = [CLint_i, KbBR, KbMU, KbAD, KbBO, KbRB] \quad (9)$$

$$\log(CLint_i) = N(\log(\hat{CLint}_i), \omega^2) \quad (10)$$

$c_{ij}$  and  $t_{ij}$ =plasma concentration and time for subject  $i$  at timepoint  $j$ ;  $\hat{c}_{ij}$ =mean of plasma concentrations;  $f_{PBPK}$ =PBPK model;  $D$ =dose;  $p$ =parameters;  $\theta$ =parameters to be estimated;  $v$ =fixed parameters; CLint=intrinsic clearance;  $\hat{CLint}$ =mean of CLint; KbBR, KbMU, KbAD, KbBO, and KbRB=partition coefficients for brain, muscle, adipose, bone, and rest of body, respectively;  $\omega^2$ =variance for CLint intersubject variability;  $\sigma$ =residual error;  $N()$ =normal distribution.

#### Prior Distributions:

$$\hat{CLint} = \text{lognormal}(7.1, 0.25^2) \quad (11)$$

$$KbBR = \text{lognormal}(1.1, 0.25^2) \quad (12)$$

$$KbMU = \text{lognormal}(0.3, 0.25^2) \quad (13)$$

$$KbAD = \text{lognormal}(2.0, 0.25^2) \quad (14)$$

$$KbBO = \text{lognormal}(0.03, 0.25^2) \quad (15)$$

$$KbRB = \text{lognormal}(0.3, 0.25^2) \quad (16)$$

$$\omega = \text{half-Cauchy}(0.0, 0.5) \quad (17)$$

$$\sigma = \text{half-Cauchy}(0.0, 0.5) \quad (18)$$

## Results

The Bayesian PBPK modeling frameworks successfully and accurately inferred the posterior distributions of the parameters of interest (Figures 3 and 5), and diagnostics showed that model predictions well characterized the observed data (Figures 2 and 4). The estimates from the three implementations were comparable (Table 1). As an example, the posterior distribution for intrinsic clearance (CLint) had medians of 1404, 1403, and 1385 L/h for the general and linear ODE (Stan/Torsten), and the general ODE (SciML/Turing.jl) applications, respectively. Given the composability of Julia packages, it was possible to use the same ODE model definition for the Bayesian analysis, sensitivity analysis and population simulations that explored an alternative dosing scenario (Figures 6 and 7).

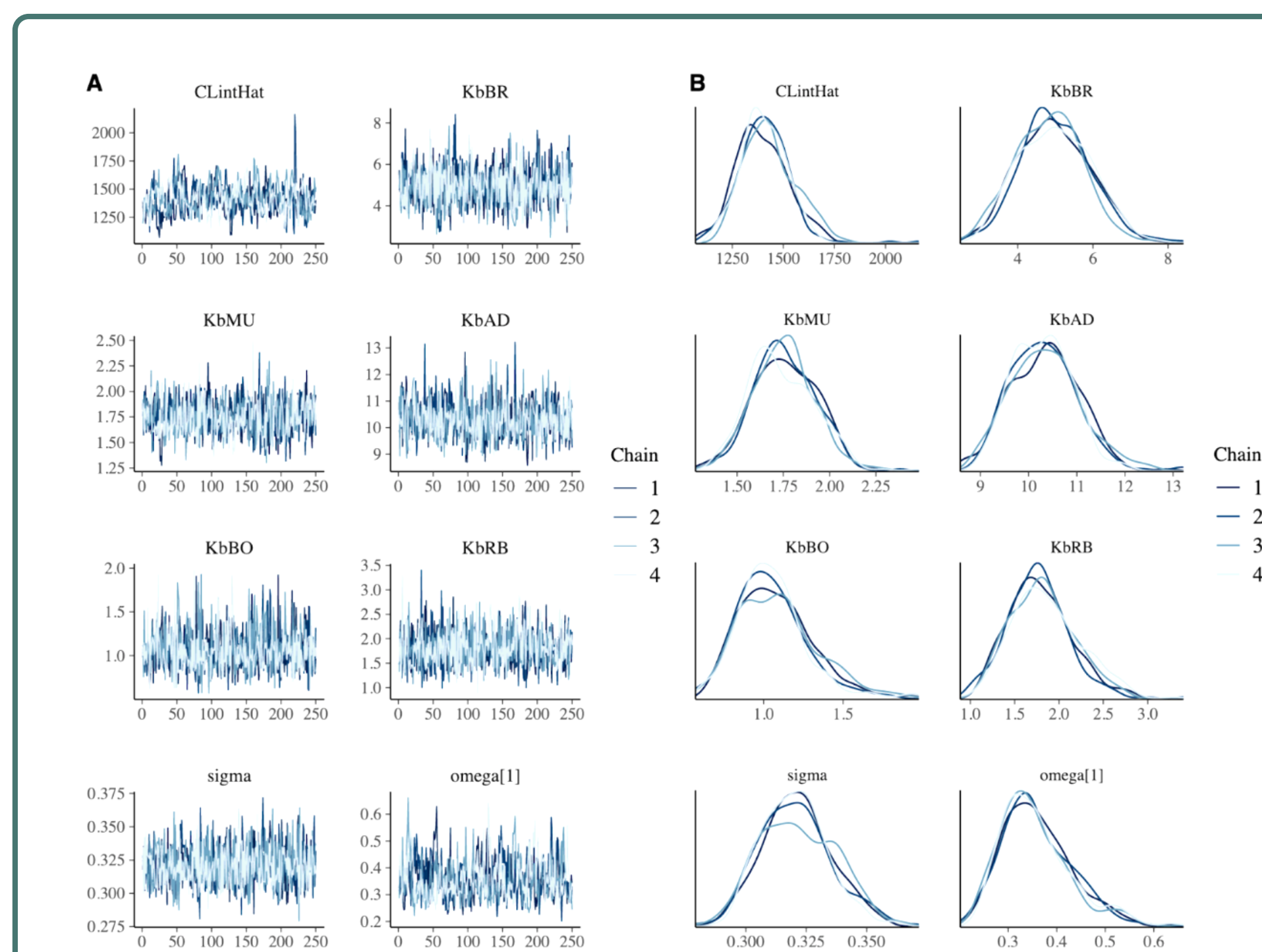


**Figure 2. (A) Trace and (B) density plots for the Torsten General ODE Application.** CLintHat=intrinsic clearance mean; Kb=partition coefficient; omega[1]=variance on CLint intersubject variability; sigma=residual error.

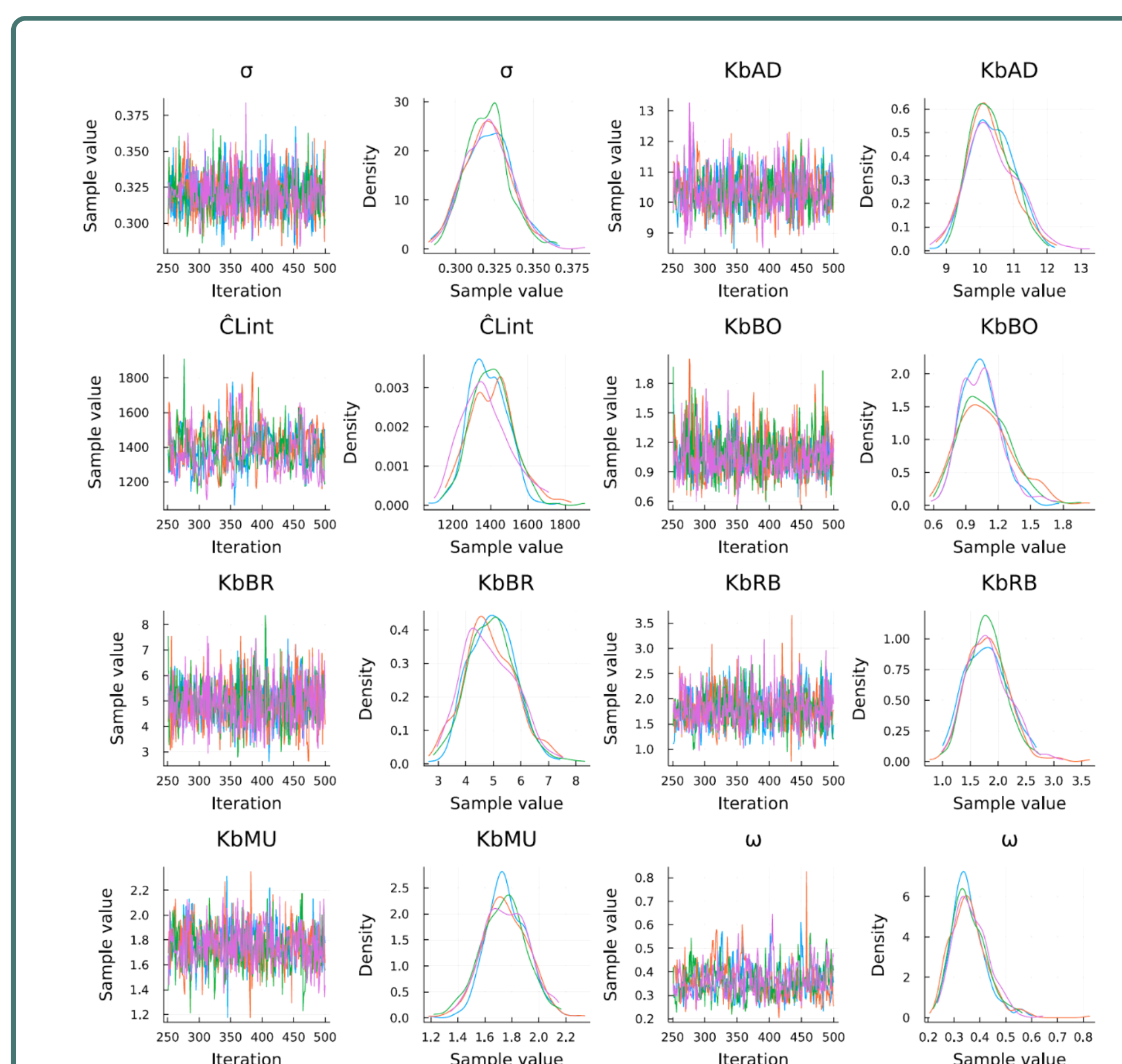


**Figure 4. Trace and Density Plots for the Turing.jl General ODE Application.** CLint=intrinsic clearance mean; Kb=partition coefficient; omega=variance on CLint intersubject variability; sigma=residual error.

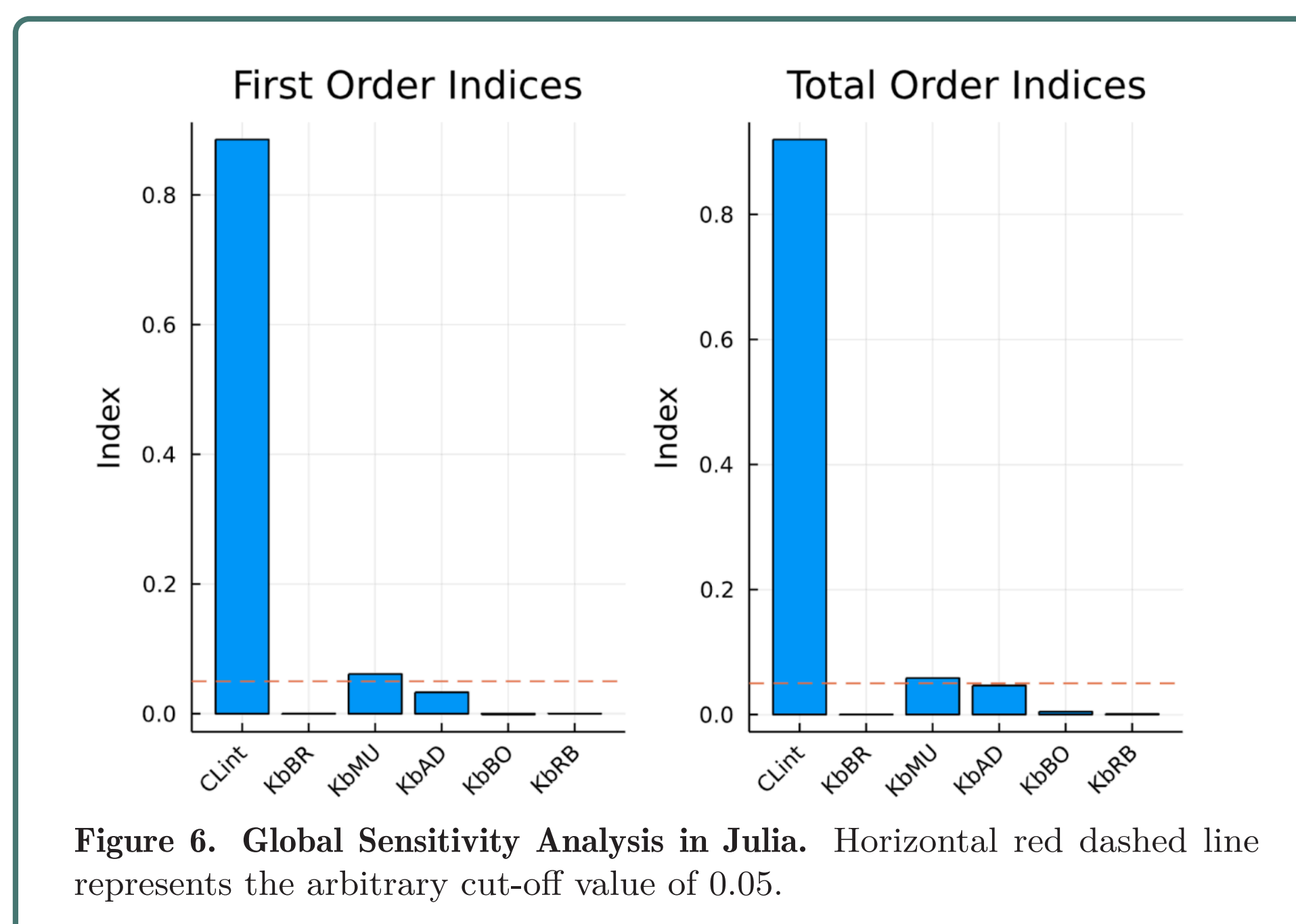


**Figure 6. Global Sensitivity Analysis in Julia.** Horizontal red dashed line represents the arbitrary cut-off value of 0.05.

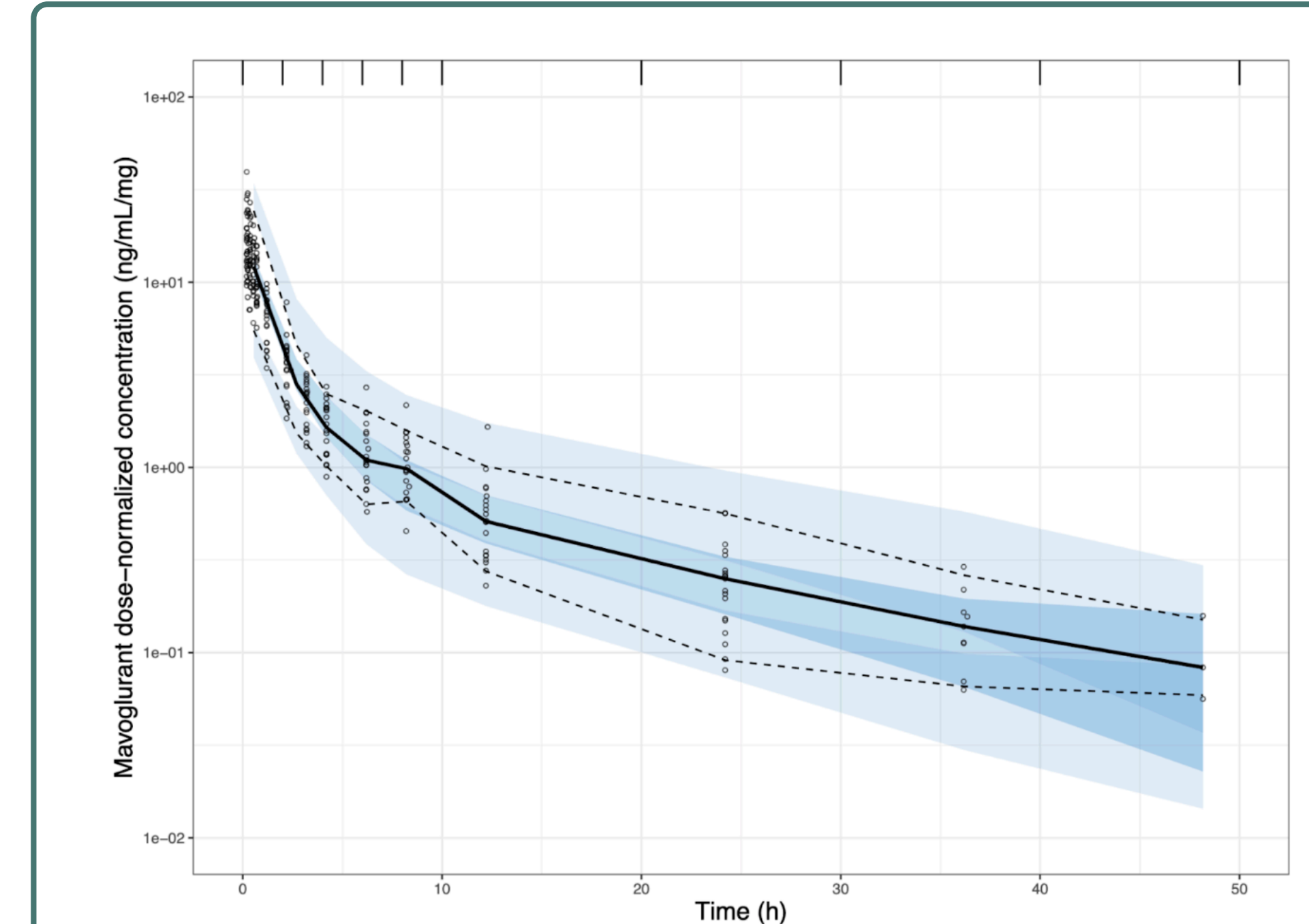


**Figure 3. Posterior Predictive Check (PPC) for the Torsten General ODE Application.** Open circles represent observed data. Solid and dashed lines represent median, 5th, and 95th percentiles of observed data. Dark and light blue bands represent 95% credible intervals around the median, 5th, and 95th percentiles of model prediction.

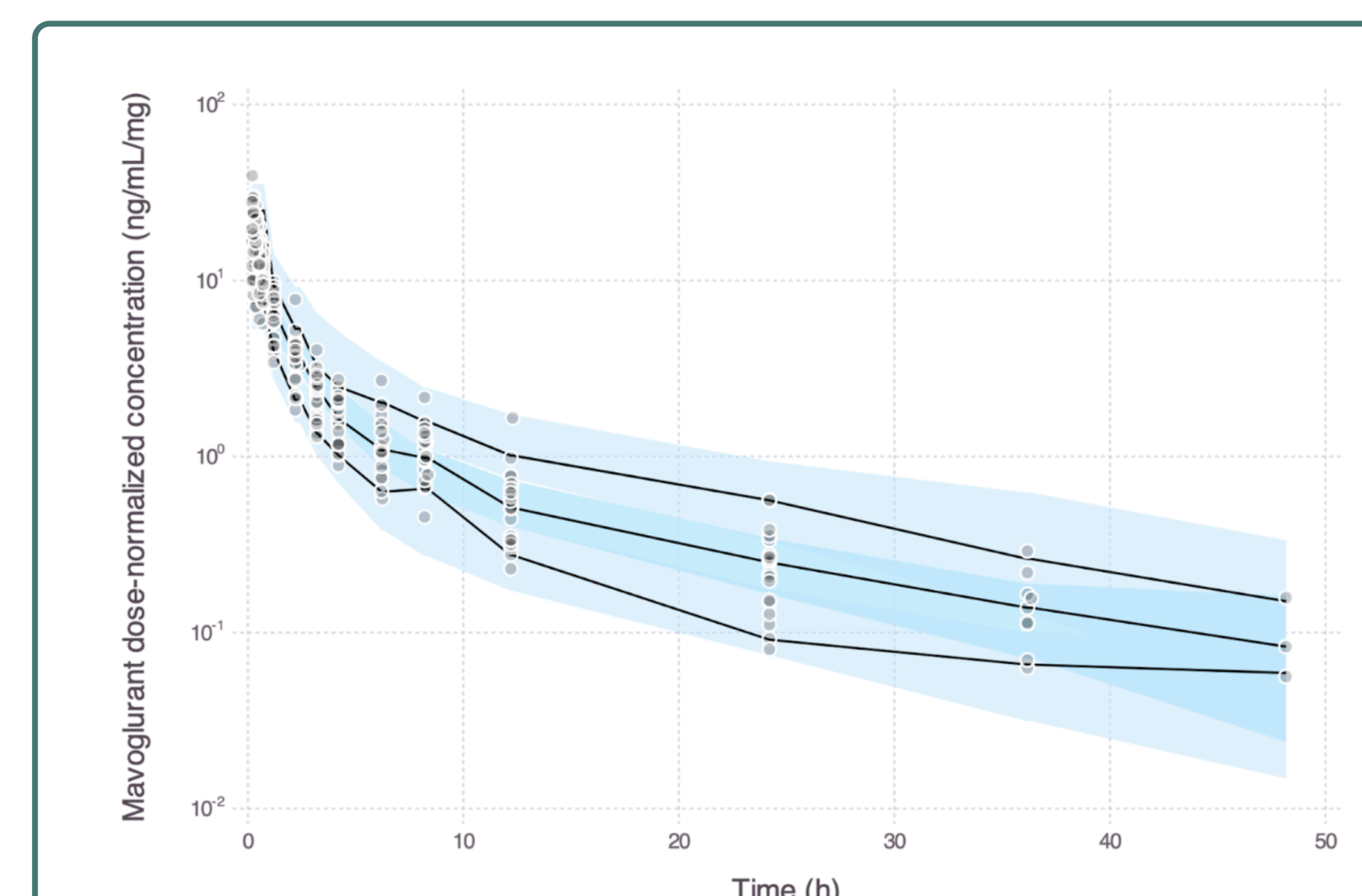


**Figure 5. Posterior Predictive Check (PPC) for the Turing.jl General ODE Application.** Circles represent observed data. Solid lines represent median, 5th, and 95th percentiles of observed data. Dark and light blue bands represent 95% credible intervals around the median, 5th, and 95th percentiles of model prediction.

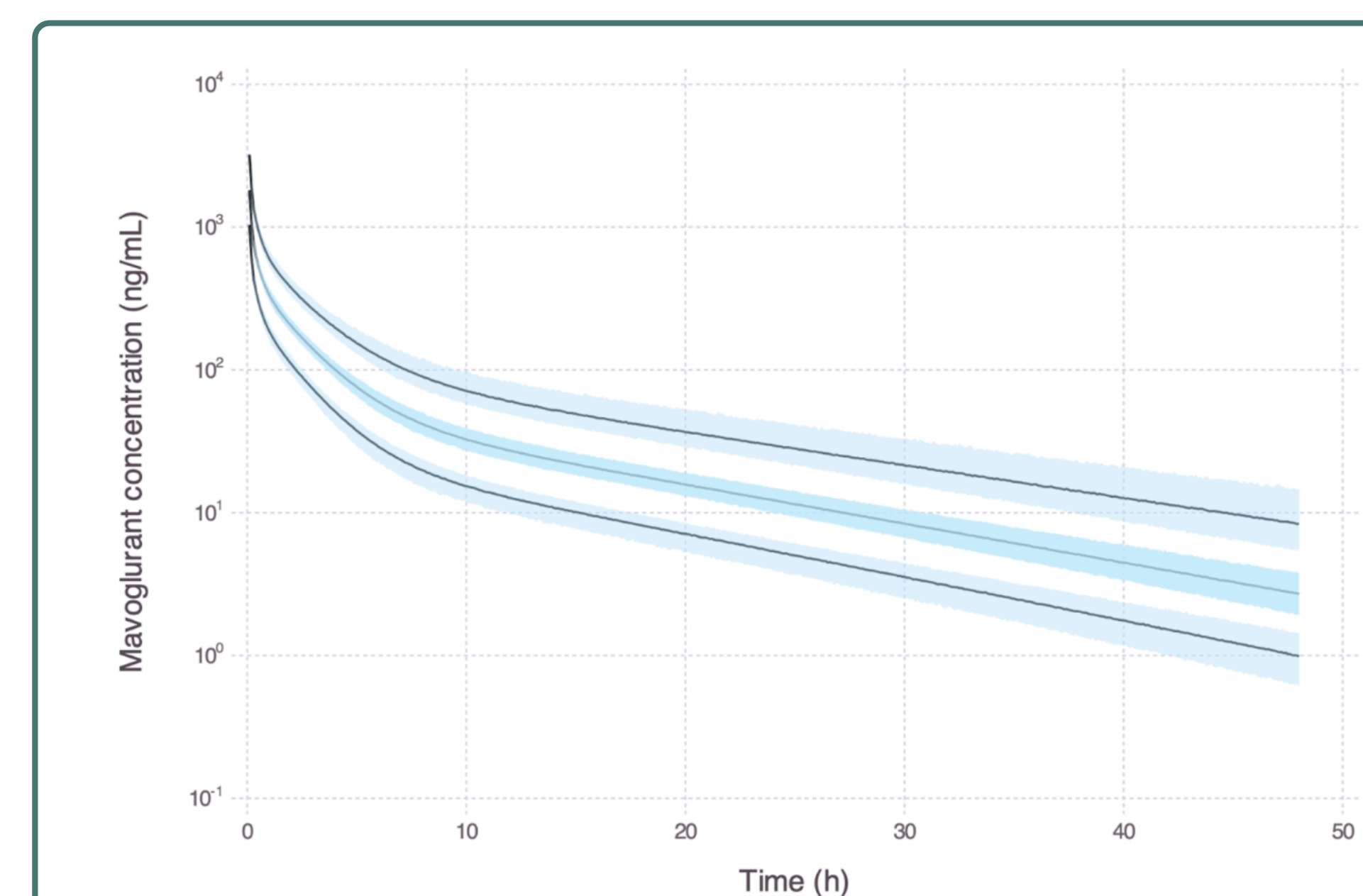


**Figure 7. PBPK Model Simulation in Julia (500 subjects x 500 replicates).** Dose administered was a single 50 mg IV infusion of mavoglurant with a rate of 300 mg/h. Solid lines represent median, 5th, and 95th percentiles of model predictions. Blue bands represent 95% credible intervals around the different percentiles.

**Table 1. Parameter estimates summary**

Parameter	Median (90% CI)		
	Stan/Torsten (general ODE solver)	Stan/Torsten (linear ODE solver)	Turing.jl
CLintHat/ $\hat{CLint}$ (L/h)	1404 (1226, 1614)	1403 (1224, 1596)	1385 (1210, 1597)
KbBR	4.93 (3.5, 6.54)	4.86 (3.46, 6.53)	4.86 (3.51, 6.41)
KbMU	1.74 (1.48, 2.03)	1.75 (1.47, 2.03)	1.75 (1.49, 2.03)
KbAD	10.3 (9.26, 11.46)	10.3 (9.33, 11.5)	10.3 (9.32, 11.49)
KbBO	1.04 (0.75, 1.49)	1.04 (0.752, 1.46)	1.05 (0.75, 1.46)
KbRB	1.78 (1.25, 2.44)	1.79 (1.25, 2.42)	1.79 (1.25, 2.44)
omega[1]/ $\omega$	0.346 (0.257, 0.501)	0.35 (0.271, 0.469)	0.35 (0.26, 0.48)
sigma/ $\sigma$	0.32 (0.299, 0.347)	0.32 (0.298, 0.342)	0.32 (0.3, 0.346)

CI = credible interval; CLintHat and  $\hat{CLint}$  = population intrinsic clearance; KbBR, KbMU, KbAD, KbBO, and KbRB are the brain, muscle, adipose, bone, and rest of body tissue:plasma partition coefficients, respectively; omega[1] and  $\omega$  = standard deviation of CLint intersubject variability; sigma and  $\sigma$  = residual error.

## Conclusion

The current work demonstrated open-source workflows to build Bayesian population PBPK models. The general applicability of the approaches discussed here makes them valuable tools for investigators interested in building Bayesian population PBPK models in an efficient, flexible, and convenient way.

## References

- Wendling, T., Dumitras, S., Ogungbenro, K. and Aarons, L. Application of a Bayesian approach to physiological modelling of mavoglurant population pharmacokinetics. *J. Pharmacokinet. Pharmacodyn.* **42** (2015):639–657.
- Fidler, M., Wilkins, J.J., Hooijmaijers, R., Post, T.M., Schoemaker, R., Trame, M.N., Xiong, Y. and Wang, W. Nonlinear mixed-effects model development and simulation using nlmixr and related R open-source packages. *CPT Pharmacometrics Syst. Pharmacol.* **8** (2019):621–633.

## Author Note

Yi Zhang was affiliated with Metrum Research Group at the time this work was conducted and is currently affiliated with Sage Therapeutics, Seattle, WA, USA.